HHS Public Access

Author manuscript

Lab Chip. Author manuscript; available in PMC 2015 April 06.

Published in final edited form as:

Lab Chip. 2012 September 21; 12(18): 3348–3355. doi:10.1039/c2lc40805h.

Modular microfluidic system fabricated in thermoplastics for the strain-specific detection of bacterial pathogens†

Yi-Wen Chen[a], **Hong Wang**[b], **Mateusz Hupert**[b], **Makgorzata Witek**[b], **Udara Dharmasiri**[a], **Maneesh R. Pingle**[c], **Francis Barany**[c], and **Steven A. Soper**[b,d,e]

Steven A. Soper: ssoper@unc.edu

[a]Department of Chemistry and Louisiana State University, Baton Rouge, LA, 70803

[b]Department of Biomedical Engineering University of North Carolina, Chapel Hill, NC, 27599

[c]Weill Cornell Medical College, New York, NY

[d]Department of Chemistry University of North Carolina, Chapel Hill, NC, 27599

[e]Nano-bioscience and Chemical Engineering, Ulsan National Institute of Science and Technology, Ulsan, South Korea

Abstract

The recent outbreaks of a lethal *E. coli* strain in Germany have aroused renewed interest in developing rapid, specific and accurate systems for detecting and characterizing bacterial pathogens in suspected contaminated food and/or water supplies. To address this need, we have designed, fabricated and tested an integrated modular-based microfluidic system and the accompanying assay for the strain-specific identification of bacterial pathogens. The system can carry out the entire molecular processing pipeline in a single disposable fluidic cartridge and detect single nucleotide variations in selected genes to allow for the identification of the bacterial species, even its strain with high specificity. The unique aspect of this fluidic cartridge is its modular format with task-specific modules interconnected to a fluidic motherboard to permit the selection of the target material. In addition, to minimize the amount of finishing steps for assembling the fluidic cartridge, many of the functional components were produced during the polymer molding step used to create the fluidic network. The operation of the cartridge was provided by electronic, mechanical, optical and hydraulic controls located off-chip and packaged into a small footprint instrument (1 ft^3). The fluidic cartridge was capable of performing cell enrichment, cell lysis, solid-phase extraction (SPE) of genomic DNA, continuous flow (CF) PCR, CF ligase detection reaction (LDR) and universal DNA array readout. The cartridge was comprised of modules situated on a fluidic motherboard; the motherboard was made from polycarbonate, PC, and used for cell lysis, SPE, CF PCR and CF LDR. The modules were task-specific units and performed universal zip-code array readout or affinity enrichment of the target cells with both made from poly(methylmethacrylate), PMMA. Two genes, *uidA* and *sipB*/*C*, were used to discriminate between *E. coli* and *Salmonella*, and evaluated as a model system. Results

†Electronic Supplementary Information (ESI) available. See DOI: 10.1039/c2lc40805h

Correspondence to: Steven A. Soper, ssoper@unc.edu.

showed that the fluidic system could successfully identify bacteria in <40 min with minimal operator intervention and perform strain identification, even from a mixed population with the target of a minority. We further demonstrated the ability to analyze the *E. coli* O157:H7 strain from a waste-water sample using enrichment followed by genotyping.

Introduction

Bacterial detection and identification play a significant role in the surveillance of food/water safety, environmental quality, public health and potential patient infections. For example, diseases caused by eating contaminated food or beverages account for an estimated 76 million illnesses, 325,000 hospitalizations and 5,000 deaths annually in the United States alone.[1–3] In addition, the Center for Disease Control has estimated that medical expenses and productivity losses resulting from these diseases total nearly $5–$6b.[4,5] Recently, an outbreak of Shiga toxin 2 (*stx2*)-positive, and intimin (*eae*)-negative Shiga toxin-producing *E. coli* (STEC) O104:H4 in Germany resulted in the death of 15 people and thousands were taken ill in a time period of one month.[6,7] Therefore, the rapid, specific and accurate detection of pathogens is crucial for the prevention of pathogen-related disease outbreaks and facilitating disease management as well as containment of suspected contaminated food and/or water supplies.

Conventionally, culturing and immunological techniques have been utilized for bacterial detection.[8,9] These methods, while simple and inexpensive, take extended periods of time to secure results and lack the specificity (*i.e.*, strain identification) when compared to molecular methods that utilize DNA to identify the bacterial species and/or strains.[10–14]

Although molecular methods represent a significant improvement over traditional culturing methods, sophisticated laboratory equipment and extensively trained personnel are required to ensure accurate, reliable and reproducible results, which prohibit the widespread implementation of these valuable techniques into a variety of settings, in particular 3rd world countries. The challenge with DNA analyses is that the processing pipeline involves many individual steps, such as cell lysis, DNA extraction and purification, PCR amplification of selected gene fragments, the specific identification of sequence variations and the readout of the results, preferably in a multiplexed fashion.

Recent advances in microfluidic-based technologies have realized the development of molecular analysis systems that incorporate many of the aforementioned processing steps for nucleic acid analyses onto a monolithic platform, which can provide process automation eliminating the need for extensive operator expertise, generate results quickly and reduce assay cost. Several demonstrations of microfluidic systems for DNA analyses have been described. For example, Burns *et al.*[15] fabricated a nanoliter DNA analyzer on a monolithic silicon wafer possessing not only the fluidic elements, but optical elements as well. Lagally and coworkers reported a portable microsystem fabricated in a glass wafer for pathogen detection and genotyping directly from *E. coli* and *S. aureus* cells.[16] The system contained a single 200-nL PCR amplification chamber connected to a micro-capillary electrophoresis, mCE, device. The commonality associated with these systems is that they employed either Si or glass as the substrate material. The challenge with glass-based systems is that extensive

lithography steps must be employed to fabricate each chip. This production format hampers the ability to generate low-cost systems that can be manufactured in a high production mode appropriate for onetime use applications.

To circumvent the need for employing glass as a substrate for the fluidic network, thermoplastics can be utilized, which can use chip fabrication techniques conducive to high rates of production.[17–20] Building on this premise, several groups have reported polymer-based systems that can analyze genetic material. For example, a monolithic system, which integrated PCR and DNA microarrays, was described by Liu *et al.*[21] The chip was fabricated in PC using CO_2 laser machining with the system employed for the analysis of both *E. coli* and *Enterococcus faecalis*. Liu and coworkers also fabricated a polymer-based system with integrated cell isolation and lysis units; PCR amplification and electrochemical microarray detection was demonstrated.[22] The system was machined into a PC substrate and capable of detecting *E. coli* in 3.5 h. Koh *et al.*[23] demonstrated a microsystem fabricated in poly(cyclic olefin copolymer), COC, which contained a PCR device directly interfaced to mCE to sort PCR products generated from different strains of *E. coli*. In another report, researchers developed a system for the analysis of bacterial DNA using COC with the fluidic structures milled into the chip.[24]

While the above examples of polymer microfluidic systems are attractive in demonstrating the utility of thermoplastics for generating low-cost systems for DNA processing, they do have some concerns including the extensive amount of post-processing required after fabrication of the desired fluidic structures, which can significantly reduce the production rate of chips. Examples of post-fabrication processing steps include the lithographic patterning of electrodes onto the fluidic chip,[21] generation of porous polymer monoliths containing silica for DNA extraction,[24] integration of wax or gel-based valves,[22,23] or the addition of magnetic beads.[22]

These fluidic systems were also made from a single material by positioning all of the functional devices onto a monolithic wafer. Unfortunately, certain materials, especially polymers, may or may not be optimal for the intended processing step. For example, some polymeric materials are appropriate for fluorescence detection and some are not due to the level of autofluorescence they generate.[25] Also, some polymers show non-specific adsorption artifacts that can produce problems for securing good contrast for microarray measurements.[26,27]

In this work, we focused on addressing the aforementioned issues by constructing an integrated polymer-based, modular microfluidic system for the rapid and efficient identification of bacterial pathogens. The system was based on a modular design approach, in which certain steps of the molecular processing pipeline were situated on modules made from a material selected to suite the particular application need. In addition, the fluidic modules were made *via* hot embossing that not only generated the fluidic network, but a number of other functional elements, such as a SPE bed[28,29] and air-embedded waveguide,[30] minimizing the number of post-processing steps required to create the system. The assay employed in this work for detecting reporter sequences within the DNA isolated

from bacterial cells consisted of a primary PCR followed by allele-specific ligation (ligase detection reaction, LDR) with readout *via* a low-density universal array.[31,32]

All of the molecular processing, from sample reception to readout, was performed on a programmable and modular fluidic cartridge. The sequence of sample processing steps performed included cell enrichment using a polyclonal antibody, cell lysis, SPE of genomic DNA (gDNA) from the whole cell lysate, PCR, LDR and universal DNA microarray readout. The fluidic cartridge was composed of functional modules connected to a fluidic motherboard. Based on material properties to optimize each molecular processing step, the motherboard was made from PC and consisted of cell lysis, SPE, PCR and LDR due to its ability to specifically extract DNAs from cell lysates and its high glass transition temperature (Tg). The array and enrichment modules were made from PMMA because of its low autofluorescence and its propensity to show minimal amounts of non-specific adsorption as well as the ability to covalently attach biomolecules to its surface following UV or plasma activation.[33–37]

We have recently reported a modular system made from thermoplastics that was used for molecular genotyping *Mycobacterium tuberculosis* directly from sputum samples.[20] Due to the relatively high levels of bacterial cells found in the sputum sample, cell enrichment prior to the molecular analysis was not required. In the case of bacterial pathogens in water samples, US EPA allowable levels of the *E. coli* O157:H7 strain are 0, 200, and 1,000 cfu per 100 ml of drinking, swimming, and recreational (boating) waters, respectively.[38] Enrichment of the cells by processing relatively large input volumes must be undertaken to accommodate the readout phases of the measurement. Therefore, we could add a cell enrichment module to our integrated system to allow for pre-concentration prior to the analysis when necessary. The enrichment module was made from PMMA and consisted of parallel channels decorated with polyclonal antibodies for the specific bacterial species (*i.e.*, *E. coli*) targeted for analysis with the strain identification affected by the molecular genotyping. To evaluate the performance of our system, enrichment of a water sample using affinity selection, a duplexed PCR, multiplexed LDR followed by universal zip-code array readout were used to detect *E. coli* strains using two genes, *uidA* and *sipB*/*C*.

Results and discussion

Architecture of the modular system

The modular design approach adopted herein offered some attractive advantages. For example, the modules and motherboard were made from a particular thermoplastic material selected to optimize processing step(s) poised on them. The motherboard was made from PC and used for SPE and thermal processing (cell lysis, PCR and LDR) while the array and enrichment modules were made from PMMA and contained an air-embedded planar waveguide or a network of fluidic channels decorated with polyclonal antibodies, respectively. We chose PC as the material for the motherboard due to its unique characteristics to allow for the specific condensation of nucleic acids to its photo-activated surface.[28] PC also has a relatively high Tg to allow it to withstand the sustained high operating temperatures required for the thermal reactions. On the other hand, the material for construction of the array module was PMMA because PMMA has significantly lower

amounts of autofluorescence compared to PC[39] as well as minimal non-specific adsorption artifacts.[40] For the enrichment module, PMMA was selected as well due to its ability to be functionalized using UV or plasma activation, generating a high density of carboxylic acid functional groups to allow for antibody attachment.[33–37] The hybrid modular approach we present herein is unique compared to other modular-based designs by its flexibility in fluidic cartridge design, ease of module interchange to accommodate the specific application needs, choice of material selection for particular modules, and the diverse array of fabrication techniques that can be employed to generate the prerequisite modules.[41,42]

The modular fluidic cartridge consisted of six devices with different functions (see Fig. 1) with an optional cell enrichment module.

(1) Enrichment module to affinity select target cells from the input sample when the cell abundance was low (see Fig. S1).

(2) A cell lysis unit that thermally lysed cells at 96 °C.

(3) A solid-phase extraction device for the purification of gDNA from a whole cell lysate using an extraction bed composed of UV activated micropillars. The SPE device was populated with an array of 3,600 50 μm diameter pillars.[27] The SPE bed possessed a total surface area of 33.6 mm^2 and the DNA load capacity was estimated to be ~242 ng. Nucleic acids were selectively immobilized onto the photo-activated PC surface, which contained carboxylate groups generated *via* UV irradiation, using an immobilization buffer containing PEG, NaCl and ethanol. After cleanup using ethanol, purified and concentrated nucleic acids were eluted from the PC surface with water or a PCR buffer. The PC-SPE method did not require magnetic beads or the loading of microchannels with beads.[28,29,43]

(4/5) CF thermal reactors for PCR and LDR. Compared to batch-type thermal cycling reactors, the CF format offers some unique advantages: (a) Better thermal management because the system is brought to thermal equilibrium prior to the start of the reactions; (b) the speed of the thermal cycling reactions (PCR and LDR) are limited only by enzyme kinetics not by heating-cooling rates,[31,44] providing extremely short reaction times; (c) no need for containment valves; and (d) the number of cycles or the time of the thermal reaction can be controlled by the length of the reaction channel and the linear transport rate through the reaction zone.[45] In addition, several thermal management strategies were utilized to give a uniform temperature distribution throughout a particular thermal zone. For example, insulating grooves between temperature zones on the back-side of the fluidic motherboard were designed to increase the thermal resistance to lateral heat conduction between zones.[46] Heating of the thermal reaction domains was carried out by placing a high thermal conductivity material, such as Cu blocks, between the heating elements and the motherboard for precise temperature control. A thin PC substrate was used to minimize the thermal capacitance of the heated area. To prolong residence time in the extension or ligation zones and reduce thermal reactor footprint, a dual-depth serpentine channel geometry (200 μm and 100 μm) was included for both CF PCR and CF LDR. The larger channel cross section in the extension/ligation zones provided a longer residence time in these zones without the need for changing the volumetric flow rate.

(6) Universal array module. An air-embedded waveguide associated with a laser-coupling prism for laser-induced fluorescence evanescent excitation of the universal array were integrated into a single microfluidic module.[30] Optical detection of the array elements was achieved with a home-built fluorescence reader consisting of a laser diode and a high sensitivity CCD camera (see Fig. S2). Evanescent excitation offered high spatial resolution and a large field-of-view (12 mm × 3 mm), allowing for imaging of the entire array without requiring scanning. Microfluidically addressed arrays typically show faster hybridization kinetics compared to their macro-scale counterparts,[27] and reduce non-specific signal and background artifacts.[47] In addition, due to the Tg of PMMA, low temperatures could be used to thermally assemble the cover plate to the fluidic substrate without chemically damaging DNA probes spotted onto its surface prior to thermal fusion bonding using conventional spotting equipment (see Fig. S3).

The PC motherboard and modules were assembled in a 3-dimensional architecture using simple and robust fluidic interconnects, which consisted of two conically-shaped holes placed on the back-sides of both the motherboard and the waveguide module with connecting tubes made of a semi-rigid polymeric material (*e.g.*, Tefzel™, see Fig. 1B). Following compression sealing, the semi-rigid connecting tubing conformed to the shape of the conical holes and provided an unswept volume of ~20 nL. This interconnect was successfully tested for pressures up to 600 psi. As compared to our previous studies utilizing a PDMS elastomer as an O-ring gasket, which produced unswept volumes to 200 nL,[31] the reported interconnect provided several beneficial characteristics; (1) It was a press fit connection, which allowed for quick connection and disconnection of the modules from the motherboard; (2) no gaskets were needed, which eliminated material-sample compatibility issues; (3) the interconnect was easy to fabricate and self-aligning with a minimal unswept volume.

Detection of bacterial cells using the integrated system

To demonstrate the utility of the modular system and the assay for the detection of bacterial pathogens, the analysis of *E. coli* O157:H7 and *Salmonella*, which are among the most problematic food/water pathogens,[2,4] was used as models. For the PCR/LDR/universal array assay, a pair of *uidA*-specific primers was used to amplify a 168-bp *uidA* gene of *E. coli* strains and a pair of *sipB*/*C*-specific primers to amplify a 250-bp *sipB*/*C* gene of *Salmonella*. The conserved single nucleotide alteration in the *uidA* gene of the O157:H7 serotype (T93G) was used to differentiate *E. coli* O157:H7 from other *E coli* strains.[48–51]

Following PCR amplification of the appropriate gene fragments, which contained the identification region, the amplicons were mixed with two sets of LDR primers, common primers and discriminating primers. The discriminating primer contained a complementary zip-code sequence (cZip) at its 5′-end and a target-specific sequence at its 3′-end. In this work, the allele-specific discriminating primers for *E. coli* O157:H7 contained a G nucleotide at its 3′-terminus (cZip5-uidA-Mt, Table S1), while the discriminating primer for *E. coli* K12 had a 3′-terminus with a T nucleotide (cZip1-uidA-Wt, Table S1). The common primer was phosphorylated at its 5′-end and possessed a fluorescent dye at its 3′-end. If there was a perfect match between the locus containing the unique signature sequence of the

target and the sequence at the 3′-end of the discriminating primer, the ligase enzyme would ligate the common and the discriminating primers. The LDR product was then directed to a specific location of the universal array by the cZip sequence, which used probes serving as zip-codes (24-mer with similar T_m values, Table S1) that contained sequences not found in the target DNA. The fluorescence signal detected at the specific zip-code position of the universal array indicated the presence of the corresponding pathogen in the sample. The advantages of the PCR/LDR/universal array assay includes: (1) LDR and universal array hybridization can be configured to detect a variety of targets by simply appending the correct cZips to the discriminating primers used in the LDR step. (2) LDR combined with the universal array readout decouples the mutation discrimination step from the hybridization step, which allows for higher specificity to detect the intended sequence variation even in a high excess of DNA not harboring the intended sequence variation. (3) PCR coupled with LDR gives two independent rounds of target amplification, which can improve the signal-to-noise in the measurement.

Fig. 2 shows the results of CF LDR products hybridized to zip-code probes using the PMMA waveguide module. Zip-code probe 3 was set as the negative control, which was not complementary to *E. coli* K12, *E. coli* O157:H7 or *Salmonella* zip-code complement sequences appended to their LDR primers and thus, no fluorescence was seen from zip-code 3 probes. Zip-code probes 1, 5 and 11 were designed to target *E. coli* K12, *E. coli* O157:H7 and *Salmonella*, respectively. Our results indicated that when only *E. coli* O157:H7 was present in the sample, zip-code probe 5 produced a positive signal (Fig. 2A). When both *E. coli* O157:H7 and *Salmonella* were present in the sample, both zip-code probes 5 and 11 gave successful hybridization events as shown in the fluorescence image of Fig. 2B. When both *E. coli* O157:H7 and *E. coli* K12 were added into the sample, zip-code probes 1 and 5 generated successful hybridization signals as shown in Fig. 2C. A sample containing a mixture of *E. coli* K12, *E. coli* O157:H7 and *Salmonella* was also evaluated and each zip-code probe (1, 5 and 11) produced fluorescence signals as shown in Fig. 2D. The specificity of each zip-code to detect the appropriate target was evident from this data. For example, ligation products bearing the zip code complement sequence generated from *E. coli* O157:H7 or *E. coli* K12 did not hybridize to zip-code probe 11, which was targeted for the detection of *Salmonella*. Even when a single nucleotide variation was required to discern *E. coli* O157:H7 from *E. coli* K12, no cross-hybridization was observed.

We further tested the ability of our system for detecting the *E. coli* O157:H7 strain in the presence of large amounts of background *E. coli* K12. This is particularly important for screening O157:H7 serotypes in a high background of commensal *E. coli* because this situation is commonly found in pathogenic *E. coli* infections.[16] In this study, *E. coli* O157:H7 was mixed with *E. coli* K12 at ratios of 0 : 1, 1 : 10, 1 : 100 and 1 : 250. The *E. coli* O157:H7 and *E. coli* K12 cells containing the *uidA* gene were concurrently PCR amplified and the strains identified using LDRs consisting of two different discriminating primers (cZip1-uidA-Wt and cZip5-uidA-Mt) and one common primer (uidA-com); see Table S1. In the presence of *E. coli* O157:H7 or *E. coli* K12, matched LDR products were generated and hybridized to the appropriate locations of the universal array. Fig. 3 shows LDR products generated from *E. coli* O157:H7 and *E. coli* K12 with different mixing ratios.

When no *E. coli* cells were present in the sample, neither zip-code probe 1 or 5 produced hybridization signals as shown in Fig. 3A. When only *E. coli* K12 was present in the sample, a ligation product was generated and detected at zip-code probe 1 (Fig. 3B). Universal array signals produced from *E. coli* O157:H7 were distinguished from *E. coli* K12 at a signal-to-background ratio ≥2 with an O157:H7 to K12 ratio of 1 : 100.

Detection limit (LOD) of *E. coli* O157:H7

We evaluated the LOD in terms of the number of pathogenic cells we could detect using our assay and integrated system. To determine the LOD, the molecular assay was conducted using *E. coli* O157:H7 as the target. Fig. S4 presents a calibration plot of the fluorescence signal as a function of the starting *E. coli* O157:H7 cell number. The lowest cell number that produced a positive signal at a signal-to-noise ratio ≥2 was 100 cfu (colony forming units) of *E. coli* O157:H7. This LOD could be improved through employing any of the following strategies: (1) Generation of an SPE bed with smaller micropillars and a smaller edge-to-edge spacing that would improve DNA recovery;[52] (2) increasing the number of PCR and/or LDR thermal cycles; (3) improve the capture efficiency of the LDR products by the zip-code probes by using a shallower (<100 μm) microfluidic channel;[27] and/or (4) increasing the numerical aperture of the relay microscope objective, which would improve the amount of fluorescence collected but at the expense of reducing the field-of-view.

Analysis of *E. coli* O157:H7 in a water sample

In many cases, enrichment of the target cell is required prior to molecular analysis due to the extremely low-abundance of the target pathogenic cells.[53] Therefore, enrichment of the target cells is often required to make sure the analyzed volume contains cells. For example, the volume analyzed for our modular system is approximately 10 μL. If the abundance of the target cells is on the order of 1 cell per mL, the probability of analyzing a cell of the appropriate serotype in 10 μL is only 1.0%.

We evaluated the ability of our modular system with the addition of a cell enrichment module to analyze the *E. coli* O157:H7 serotype in a waste-water sample. The microchip enrichment procedure has been described elsewhere.[53] Briefly, waste-water (1 mL) was obtained from a purification plant in Baton Rouge and was filtered using a PCTE membrane with a 10 μm pore size to remove large particulates (*e.g.*, solid particulates and debris) from the sample. The effluent was then processed for *E. coli* using the PMMA module (Fig. S1), which was equipped with 16 curvilinear high aspect ratio microchannels covalently decorated with polyclonal anti-O157 antibodies. O157 serotypes of *E. coli* were then released from the channel surface using 5 μL of a cell-stripper solution and transferred into the integrated system for molecular analysis. *E. coli* serotypes expressing O157 antigens, including O157:H7, O157:H12, O157:H42, O157:H29, O157:H19 and O157:H45, were enriched by a factor of 2×10^2 using the enrichment module with the specific serotype confirmed *via* PCR/LDR/universal array processing.

Fig. 4 presents results showing the analysis of *E. coli* O157:H7 in a waste-water sample using our modular system. The results indicated LDR products generated and fluorescence signals produced at zip-code probe 5, which specifically interrogated for the *E. coli*

O157:H7 strain (see Fig. 4A). No fluorescence signal was seen for *E. coli* K12. A negative control sample was also performed and no *E. coli* O157:H7 signal was detected as shown in Fig. 4B. In the waste-water sample analyzed, the level of *E. coli* O157:H7 determined from the calibration plot (Fig. S4) was 9.5 ±0.3 × 10^3 cfu/mL. At this cell abundance, even without enrichment, every 10 μL sample would contain ~95 cells per sampling volume. However, the number of *E. coli* O157:H7 cells injected into the chip would be slightly less than the LOD predicating the need for the enrichment step.

Conclusions

We have developed an integrated and modular microfluidic system that consisted of modules made from PMMA and a fluidic motherboard made from PC with the material selection based on optimizing the processing step(s) poised onto the modules or motherboard. In addition, the system could be reprogrammed by adding a module for target cell enrichment if required demonstrating the flexibility in the design for accommodating changes in the assay strategy. The integrated platform utilized a CF PCR/CF LDR/universal array molecular assay for the sensitive detection of bacterial pathogens, even from waste-water samples. The use of off-chip active components reduced the complexity of the fluidic cartridge making it appropriate for one-time use applications. Also, the use of hot-embossing to fabricate passive elements, such as micropillars for the SPE, micromixers and air-embedded waveguides, in the same step to make the fluidic structures minimized the number of finishing steps to produce the final cartridge.

We demonstrated the utility of the integrated and modular system by analyzing *E. coli* and *Salmonella* bacterial pathogens in a total processing time <40 min (10 min for sample preparation, 24 min for PCR, 4 min for LDR and 20 s for image readout). The assay utilized by the system provided the ability to differentiate strains based on single nucleotide variations; discrimination between *E. coli* K12 and *E. coli* O157:H7 were demonstrated even for one O157:H7 sequence in 100 K12 sequences.

While the system was demonstrated by the analysis of *E. coli* or *Salmonella*, simple reprogramming of the primer sequences used for the PCR and LDR would allow the system to be used for the detection of any pathogenic species without requiring hardware reconfiguration, especially when used in conjunction with the universal array; the same array can be used for any bacterial species when the correct zip-code complements are appended to the LDR primers. For example, by adding PCR primers and LDR primers targeting *stx2* and *eaeA* genes and the corresponding zip-code probes, this system can easily identify the Shiga toxin 2 (*stx2*)-positive, intimin (*eae*)-negative STEC serotype O104:H4.[6]

Methods

Materials and regents

Heat-inactivated *E. coli* O157:H7 and *Salmonella* cells were purchased from Kirkegaard & Perry Laboratories (Gaithersburg, MD). Other chemicals used in these studies are listed in the Supporting Information.

Microfluidic cartridge fabrication

The modular fluidic cartridge is depicted in Fig. 1A. It consisted of the motherboard made from PC with devices for cell lysis, SPE, PCR and LDR, while one module was used for the universal array and contained a planar waveguide (Fig. 1A). The enrichment module (see Supporting information, Fig. S1) was used only for analyzing the waste-water sample. Modules were interconnected to the PC motherboard using short pieces of Tefzel™ tubing (OD = 1/16″, ID = 250 μm, Upchurch) inserted between conically-shaped holes placed on the backsides of both the motherboard and module to provide leak-free interconnections (see Fig. 1B). Details on the fabrication of the fluidic cartridge can be found in the Supporting Information.

Surface modification of PMMA and array preparation

PMMA surface modification and array preparation were carried out in a process reported previously.[30,45,54] The procedural details are given in the Supporting Information. Briefly, DNA probes were spotted onto a plasma activated PMMA surface, which also served as a waveguide, followed by thermal fusion bonding of a cover plate to the PMMA substrate.

PCR and LDR conditions

We used CF thermal cycling for several reasons including its ability to provide ultrafast cycling times ultimately limited by the kinetic rate of dNTP incorporation by the polymerase and the lack of valves required to contain the PCR mixture during thermal cycling as required for batch-type thermal cyclers.[44–46] Details of PCR and LDR conditions can be found in the Supporting Information.

Peripheral packaging and instrument operation (see Fig. S2)

The physical dimensions of this instrument were 12″ (length) × 12″ (width)×12″ (height) and included an Instrument Control Unit (ICU), actuators, pumps, solenoid valves, heating stage and solution reservoirs. Included in this footprint was also a compact optical reader used to secure fluorescence signatures from the universal zip-code array. Further details are given in the Supporting Information.

Supplementary Material

Refer to Web version on PubMed Central for supplementary material.

References

1. Archer DL, Kvenberg JE. J Food Prot. 1985; 48:887–894.
2. Mead PS, Slutsker L, Dietz V, McCaig LF, Bresee JS, Shapiro C, Griffin PM, Tauxe RV. Emerg Infect Dis. 1999; 5:607–625. [PubMed: 10511517]
3. Cohen ML. Nature. 2000; 406:762–767. [PubMed: 10963605]
4. Todd ECD. Int J Food Microbiol. 1989; 9:313–326. [PubMed: 2701860]
5. Roberts T. Am J Agr Econ. 1989; 71:468–474.
6. Askar M, Faber MS, Frank C, Bernard H, Gilsdorf A, Fruth A, Prager R, Hohle M, Suess T, Wadl M, Krause G, Stark K, Werber D. Eurosurveillance. 2011; 16:2–4.
7. http://www.euro.who.int/en/home.

8. Swaminathan B, Feng P. Annu Rev Microbiol. 1994; 48:401–426. [PubMed: 7826012]
9. Rodriguez-Mozaz S, Marco MP, de Alda MJL, Barcelo D. Pure Appl Chem. 2004; 76:723–752.
10. Hu Y, Zhang Q, Meitzler JC. Journal of Applied Microbiology. 1999; 87:867–876. [PubMed: 10664910]
11. Ibekwe AM, Watt PM, Grieve CM, Sharma VK, Lyons SR. Applied and Environmental Microbiology. 2002; 68:4853–4862. [PubMed: 12324331]
12. Chizhikov V, Rasooly A, Chumakov K, Levy DD. Applied and Environmental Microbiology. 2001; 67:3258–3263. [PubMed: 11425749]
13. Shepard JRE, Danin-Poleg Y, Kashi Y, Walt DR. Anal Chem. 2005; 77:319–326. [PubMed: 15623311]
14. Kostrzynska M, Bachand A. Can J Microbiol. 2006; 52:1–8. [PubMed: 16541153]
15. Burns MA, Johnson BN, Brahmasandra SN, Handique K, Webster JR, Krishnan M, Sammarco TS, Man PM, Jones D, Heldsinger D, Mastrangelo CH, Burke DT. Science. 1998; 282:484–487. [PubMed: 9774277]
16. Lagally ET, Scherer JR, Blazej RG, Toriello NM, Diep BA, Ramchandani M, Sensabaugh GF, Riley LW, Mathies RA. Anal Chem. 2004; 76:3162–3170. [PubMed: 15167797]
17. Becker H, Gartner C. Anal Bioanal Chem. 2008; 390:89–111. [PubMed: 17989961]
18. Soper SA, Ford SM, Qi S, McCarley RL, Kelly K, Murphy MC. Anal Chem. 2000; 72:642A–651A.
19. de Mello A. Lab on a Chip. 2002; 2:31N–36N. [PubMed: 15100858]
20. Wang H, Chen HW, Hupert ML, Chen PC, Datta P, Pittman TL, Goettert J, Murphy MC, Williams D, Barany F, Soper SA. Angewandte Chemie, International Edition. 2012; 51:4349–4353.
21. Liu YJ, Rauch CB, Stevens RL, Lenigk R, Yang JN, Rhine DB, Grodzinski P. Anal Chem. 2002; 74:3063–3070. [PubMed: 12141665]
22. Liu RH, Yang JN, Lenigk R, Bonanno J, Grodzinski P. Anal Chem. 2004; 76:1824–1831. [PubMed: 15053639]
23. Koh CG, Tan W, Zhao M, Ricco AJ, Fan ZH. Anal Chem. 2003; 75:4591–4598. [PubMed: 14632069]
24. Sauer-Budge AF, Mirer P, Chatterjee A, Klapperich CM, Chargin D, Sharon A. Lab on a Chip. 2009; 9:2803–2810. [PubMed: 19967117]
25. Shadpour H, Musyimi H, Chen JF, Soper SA. Journal of Chromatography A. 2006; 1111:238–251. [PubMed: 16569584]
26. Thomas GA, Farquar HD, Sutton S, Hammer RP, Soper SA. Molecular Review Diagnostics. 2002; 2:429–447.
27. Wang Y, Vaidya B, Farquar HD, Stryjewski W, Hammer RP, McCarley RL, Soper SA, Cheng YW, Barany F. Anal Chem. 2003; 75:1130–1140. [PubMed: 12641233]
28. Witek MA, Llopis S, Wheatley A, McCarley R, Soper SA. Nucleic Acids Research. 2006; 34:e74. [PubMed: 16757572]
29. Witek MA, Hupert ML, Park DSW, Fears K, Murphy MC, Soper SA. Anal Chem. 2008; 80:3483–3491. [PubMed: 18355091]
30. Xu F, Datta P, Wang H, Gurung S, Hashimoto M, Wei S, Goettert J, McCarley RL, Soper SA. Anal Chem. 2007; 79:9007–9013. [PubMed: 17949012]
31. Hashimoto M, Hupert ML, Murphy MC, Soper SA, Cheng YW, Barany F. Anal Chem. 2005; 77:3243–3255. [PubMed: 15889915]
32. Hashimoto M, Barany F, Soper SA. Biosens Bioelectron. 2006; 21:1915–1923. [PubMed: 16488597]
33. Wei SY, Vaidya B, Patel AB, Soper SA, McCarley RL. Journal Of Physical Chemistry B. 2005; 109:16988–16996.
34. McCarley RL, Vaidya B, Wei SY, Smith AF, Patel AB, Feng J, Murphy MC, Soper SA. Journal of the American Chemical Society. 2006; 127:842–843. [PubMed: 15656615]
35. Xu F, Datta P, Wang H, Gurung S, Hashimoto M, Wei SY, Goettert J, McCarley RL, Soper SA. Anal Chem. 2007; 79:9007–9013. [PubMed: 17949012]

36. Balamurugan S, Obubuafo A, Soper SA, Spivak DA. Analytical and Bioanalytical Chemistry. 2008; 390:1009–1021. [PubMed: 17891385]
37. Subramanian B, Kim N, Lee W, Spivak DA, Nikitopoulos DE, McCarley RL, Soper SA. Langmuir. 2011; 27:7949–7957. [PubMed: 21608975]
38. Keene WE, McAnulty JM, Hoesly FC, Williams LP Jr, Hedberg K, Oxman GL, Barrett TJ, Pfaller MA, Fleming DW. N Engl J Med. 1994; 331:579–584. [PubMed: 8047082]
39. Wabuyele MB, Ford SM, Stryjewski W, Barrow J, Soper SA. Electrophoresis. 2001; 22:3939–3948. [PubMed: 11700724]
40. Xu YC, Vaidya B, Patel AB, Ford SM, McCarley RL, Soper SA. Anal Chem. 2003; 75:2975–2984. [PubMed: 12964741]
41. Lin F, Sherman P, Li D. Biomedical Microdevices. 2004; 6:125–130. [PubMed: 15320634]
42. Shaikh KA, Suk Ryu K, Goluch ED, Nam J-M, Liu J, Thaxton CS, Chiesl TN, Barron AE, Lu Y, Mirkin CA, Liu C. PNAS. 2005; 102:9745–9750. [PubMed: 15985549]
43. Wang H, Chen JF, Zhu L, Shadpour H, Hupert ML, Soper SA. Anal Chem. 2006; 78:6223–6231. [PubMed: 16944905]
44. Hashimoto M, Chen PC, Mitchell MW, Nikitopoulos DE, Soper SA, Murphy MC. Lab on a Chip. 2004; 4:638–645. [PubMed: 15570378]
45. Chen JF, Wabuyele M, Chen HW, Patterson D, Hupert M, Shadpour H, Nikitopoulos D, Soper SA. Anal Chem. 2005; 77:658–666. [PubMed: 15649068]
46. Chen PC, Nikitopoulos D, Soper SA, Murphy MC. Biomedical Microdevices. 2008; 10:141–152. [PubMed: 17896180]
47. Erickson D, Liu XZ, Krull U, Li DQ. Anal Chem. 2004; 76:7269–7277. [PubMed: 15595869]
48. Feng P, Lampel KA. Microbiology-Sgm. 1994; 140:2101–2107.
49. Cebula TA, Payne WL, Feng P. Journal of Clinical Microbiology. 1995; 33:248–250. [PubMed: 7535315]
50. Monday SR, Whittam TS, Feng PCH. Journal of Infectious Diseases. 2001; 184:918–921. [PubMed: 11510000]
51. Yoshitomi KJ, Jinneman KC, Weagant SD. Molecular and Cellular Probes. 2003; 17:275–280. [PubMed: 14602477]
52. Witek M, Park D, Hupert M, McCarley RL, Murphy MC, Soper SA. Anal Chem. 2008; 80:3483–3491. [PubMed: 18355091]
53. Dharmasiri U, Witek MA, Adams AA, Osiri JK, Hupert ML, Bianchi TS, Roelke DL, Soper SA. Anal Chem. 2010; 82:2844–2849. [PubMed: 20218574]
54. Situma C, Wang Y, Hupert M, Barany F, McCarley RL, Soper SA. Anal Biochem. 2005; 340:123–135. [PubMed: 15802138]

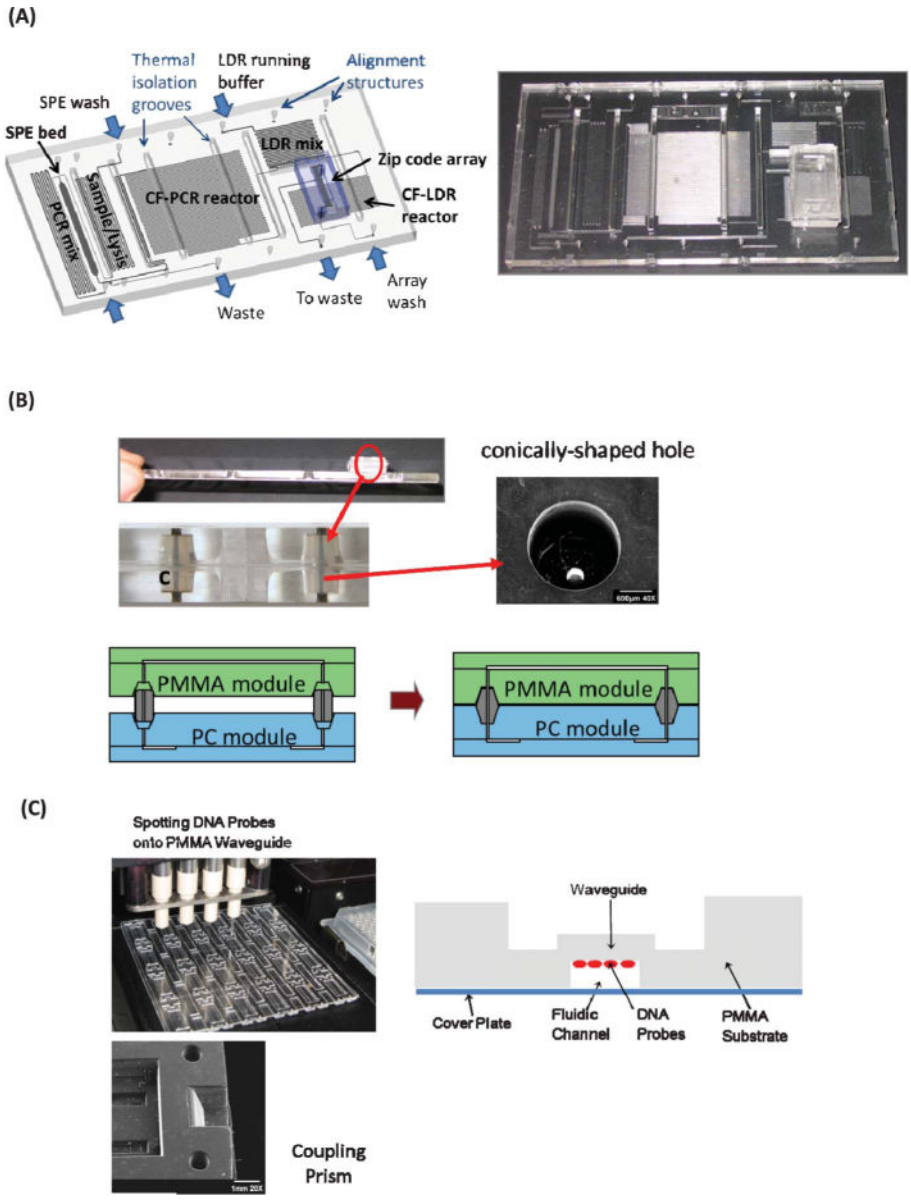

Fig. 1.

(A) A schematic of the modular fluidic cartridge as well as a photograph of an assembled cartridge. The fluidic cartridge was composed of a module(s) interconnected to a motherboard. The motherboard was made from PC and consisted of processing steps for cell lysis, SPE of gDNA, PCR and LDR, while the modules were made from PMMA. The PC motherboard was interconnected to the PMMA modules through short pieces of tubing and conically-shaped holes that were thermally embossed into the PC. (B) Schematic and optical micrograph of the motherboard-to-module fluidic interconnection. Connecting tube was placed inside a conically-shaped hole in which channels were filled with a black dye that was used for visualization (c). The micrograph to the right shows the laser drilled hole. (C) Layout of the PMMA waveguide module (right picture) consisting of the air-embedded waveguide, a coupling prism and the universal array. The waveguide and coupling prism

(see center picture) were located on the backside of the module and the front-side contained the fluidic channel, which had as its floor the waveguide. DNAs could be spotted (see picture on the left) onto the waveguide using a non-contact spotter prior to thermal fusion bonding the cover plate to this module's substrate.

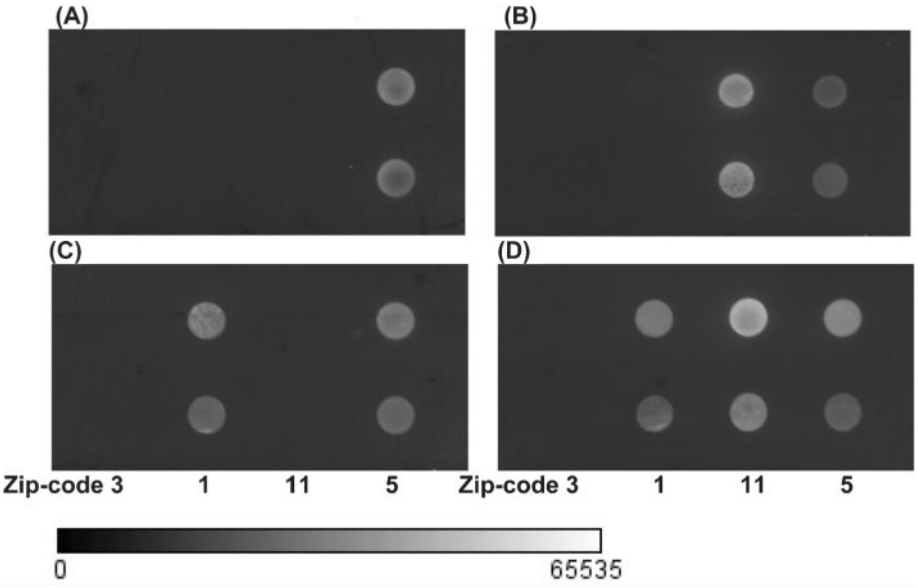

Fig. 2.

Detection of bacterial pathogens using the integrated and modular system. Fluorescence images of the universal array following CF PCR and CF LDR for a sample containing (A) *E. coli* O157:H7, (B) *Salmonella* and *E. coli* O157:H7, (C) *E. coli* K12 and *E. coli* O157:H7 and (D) *E. coli* K12, *Salmonella* and *E. coli* O157:H7. The sample flowed through the system using a volumetric flow rate of 1 μL min^{-1} for PCR and 2 μL min^{-1} for LDR and then, the arrays were imaged using the fluorescence reader with a 20 s integration time. Zip-code probe 3 was the negative control and zip-code 1, 5 and 11 probed for *E. coli* K12, *E. coli* O157:H7 and *Salmonella*, respectively. Each zip-code probe was spotted in a duplex format (top and bottom rows). While the input concentration of the bacteria used in each experiment was similar (~10 000 cfu), spot-to-spot intensity variations arose from variations in the immobilization chemistry and PCR efficiency for each bacterial species. Inclusion of internal control spots can correct for these variations. The relative standard deviation in these measurements was in the range of 8–12%.

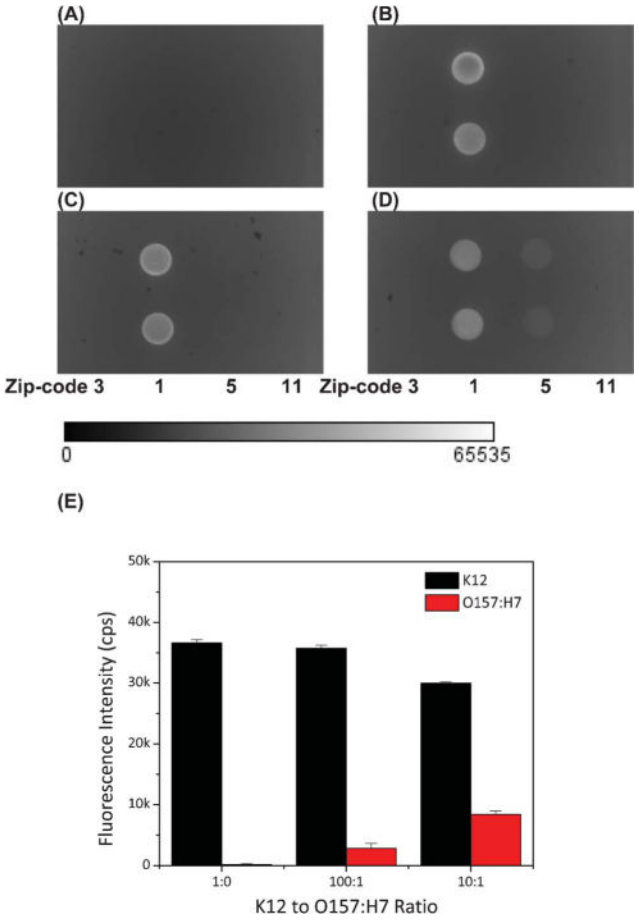

Fig. 3.

Identification of *E. coli* O157:H7 in the presence of background *E. coli* K12 with various amounts of O157:H7: (A) No DNA template; (B) K12 only (10 000 cfu); (C) K12 to O157:H7 ratio of 100 : 1 (10 000:100 cfu) and (D) K12 to O157:H7 ratio of 10 : 1 (10 000:1000 cfu). The fluorescence intensity profiles from (B), (C) and (D) are shown in (E). The error bars represent one standard deviation, which was determined from two measurements. Each zip-code probe was spotted in duplicate and is represented in each row.

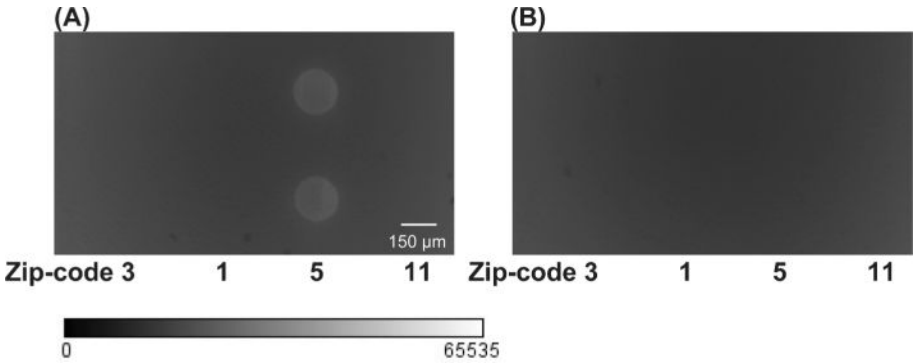

Fig. 4.

Analysis of *E. coli* O157:H7 in a waste-water sample. The fluorescence image of the array was accomplished using evanescent excitation with an integration time of 20 s following microarray hybridization for a waste-water sample with (A) *E. coli* O157:H7 present and (B) no cells present. The water sample was filtered and then enriched using the PMMA enrichment module consisting of curvilinear channels decorated with polyclonal anti-O157 antibodies. After cell enrichment, cells were released and genotyped, which effectively discriminated the O157:H7 serotype from other types of *E. coli*. Each zip-code probe was spotted in duplicate and is represented in each row.